

Diabetic Retinopathy Severity Identification Using 3D Dual-Domain Attention Approach

Benix Pearlin Moses M, R. Maria Sheeba

*¹PG Scholar, Department of CSE, Ponjesly College of Engineering, Nagercoil, India

²Professor, Department of CSE, Ponjesly College of Engineering, Nagercoil, India

ARTICLE INFO

Article History:

Accepted: 07 Sep 2023

Published: 29 Sep 2023

Publication Issue

Volume 10, Issue 5

September-October-2023

Page Number

302-311

ABSTRACT

The diabetic retinopathy (DR) is one of prominent reason of visual impairment among the people around the globe suffers from diabetes. Early and timely diagnosis of this problem can minimise the risk of proliferated diabetic retinopathy. Diabetes is caused by persistently high blood glucose levels, which leads to blood vessel aggravations and vision loss. Therefore, it becomes important to classify DR stages. An automated system for this purpose contains several phases like identification and classification of DR stages in fundus images. Deep learning techniques based on extraction of features and automatic extraction of features with a hybrid network have been presented for diabetic retinopathy detection. This method effectively identify diabetic retinopathy identification from the chest region by using the 3D Dual-Domain Attention Approach. The dual-domain attention module propised learns local and global information in spatial and context domains from encoding feature maps in Unet. Our attention module generates refined feature maps from the enlarged reception field at every stage by attention mechanisms and residual learning to focus on complex tumor regions. Experimental results show that the proposed network can identify the DR stages with high accuracy. The proposed method attains an F1-score of 91.34%, precision of 92.34%, accuracy of 98.65%, on the healthy retina, stage 1, stage 2, and stage 3 fundus images. Compared with other models, our proposed network achieves comparable performance.

Keywords : Deep Learning, Fundus Scan, Diabetic Retinopathy, Image Identification

I. INTRODUCTION

Diabetes is caused by an accumulation of glucose in the bloodstream [1]. International Diabetes Federation (IDF) have assessed that worldwide 451 million people suffers with diabetes in 2017 and they estimated that it increase to 693 million by 2045 [2]. Diabetes can lead to risky complications like a coronary episode, issues with neuropathy and nephropathy, loss of eyesight, teeth bleeding, nerve failure, lower limb seizure, stroke, heart failure, and so on [3]. Diabetic neuropathy is caused by the destruction of kidney nephrons, while diabetic retinopathy is caused by the injury in the brain neurons, which leads to retinal infection and can progressively impair eyesight at an early stage [4]. Optical coherence tomography, fundus fluorescein angiography, slit lamp biomicroscopy, and fundus imaging are some of the methods used to identify the afflicted eye [5]. The maximum increase in glucose level has a significant impact on blood vessels, causing seeping of blood from the eyes and weakening of the human visual system [6]. When the brain recognizes blood leaking, it stimulates the surrounding tissues to deal with the situation. As a result, it causes the sporadic formation of new blood vessels, but the resulting cells are anemic [7].

Retinal fundus image analysis is a helpful medical processing operation. Ophthalmologists can employ retinal blood vessel segmentation to help them diagnose a variety of eye problems [8]. Early prediction of DR can play a significant role in preventing vision loss. Further, the structural change as a result of the vascular system may provide physical signs for the disease; hence, medical specialists advise patients to receive annual retinal screening tests utilizing dilated eye exams [9]. Interestingly, these retina scans might be used to detect diabetes, although this would necessitate ophthalmologists' general judgment, which could take time.

Deep Learning techniques have demonstrated superior performance in the identification of DR, with a high level of accuracy which distinguishes them from other models. Undoubtedly, DL can uncover hidden elements in images that medical specialists would never see. Due to its capability in feature extraction and training in discriminating between multi-classes, the convolutional neural network (CNN) is the most commonly used DL approach in the medical system. On several medical datasets, the transfer learning (TL) approach has also made it easier to retrain deep neural networks quickly and reliably. The purpose of this research is to evaluate the effectiveness of hybrid neural network models for identification of DR which aids in the reduction of vision loss caused by DR and reduces the stress and time-consumption of ophthalmologists.

The remaining section of this article is outlined in the following manner: Section 2 discusses the related work of DR algorithms; Section 3 explains the method behind our suggested approach; Section 4 presents the experimental outcomes and model evaluation. Section 5 presents the discussion of our study; and lastly, a conclusion is written in Section 6.

II. LITERATURE REVIEW

Diabetic retinopathy is the most noticeable problem in diabetic patients which leads to loss of vision which can be avoided if the problem is identified and treated at a prior stage. When the problem has been diagnosed, the patient must be checked at regular intervals to know the advancement of the ailment [10]. An efficient mechanism for detecting the problem based on the patient's reports will be useful for the ophthalmologist to avoid the loss of vision due to diabetes. Researchers have designed various algorithms for the investigation of scan reports thereby to do the exact diagnosis of diabetic retinopathy [12-14] The human eye consists of optic nerves and discs. So the eye images are to be

segmented into parts for identification and categorization of DR. It can also be possible by inspecting the fundus images for the existence of hemorrhages, injuries, smaller scale aneurysms, exudates, and so forth. Deep learning plays a vital role in making the scenarios smart, i.e., making the environment smart with automation and making the medical domain also as smart with automated disease detection [15].

In the recent decade, number of automated systems have been created for the diagnosis of diabetic retinopathy [16,17]. Hence, the majorities of the researchers concentrated on automatically identify and categorize the lesions. In the paper [18], the author's Shahin et al. built up a framework to automatically categorize retinal fundus pictures as having and not having diabetic retinopathy. The authors considered morphological dispensation to retrieve necessary features like the area of the blood vessels and exudates region along with entropy and homogeneity indexes.

Kumar et al. [19] have presented an improved methodology for haemorrhage recognition and micro aneurysms that contributed to the improvement when compared to the existed methodology for identification of DR. In the methodology, an upgraded segmentation strategy was introduced for separating the blood veins and optic disc. Consequently, the task of classification was done based on a neural network system that was trained by considering the features of micro aneurysms [20]. Toward the end, the results have exhibited the advancement of the considered methodology with accuracy as the performance measure.

An algorithm for automatic identification which comprises of majorly two sections: the top-down approach to divide the exudates region and a coordinate system focused at the fovea to review the seriousness of rigid exudates. Casanova et al., in the

paper [21] presented an algorithm based on random forest technique to categorize the individuals without and with diabetic retinopathy and got an accuracy of over 90%. Quelled et al. [22] developed a framework to recognize diabetic retinopathy by utilizing a convolutional neural system (CNN) which automatically categorizes the injuries by making heatmaps which have the indications for the possibility to find novel biomarkers in the fundus pictures. They trained CNN with a collaborative learning strategy which is positioned second place in Kaggle competition on Diabetic Retinopathy [23] and acquired an outcome with the zone of 0.954 under the ROC curve on the Kaggle dataset.

Gulshan et al. [24] used a CNN model called Inception-V3 to recognize referable diabetic retinopathy given a dataset that comprises over 128,000 fundus pictures. Because of huge training data and a very well separation of fundus pictures, the model accomplished a good performance with a metric area under curve. Gargeya and Leng [25] projected a technique that integrates deep CNN with customary algorithms of machine learning. In the projected technique, after the pre-processing of the fundus images, they are considered as inputs to a residual network. To the result of the fundus images from the last pooling layer, a few metadata factors are added and are considered as input to a classifier named decision tree classifier to have the separation among normal fundus images and a fundus image with Diabetic retinopathy.

Our paper focuses on the problem of low-quality DR images. The novelty of our proposed model is in threefold. First, the dual channels of fundus images which are images utilized for DR identification because of their interconnected properties. Secondly, the fine-tuning techniques are utilised for better extraction of features. Lastly, the output weights of each channel are merged for a robust prediction

result. Public datasets belonging to Messidor are used to evaluate the performance of our research.

III. MATERIALS AND METHODS

The procedure of the proposed approach in this paper is discussed in the subsequent subsections. In this section, details about the dataset, pre-processing steps, and implementation detail of the proposed method are discussed. Further, this section discusses the proposed 3D Dual-Domain Attention architecture and details of the loss functions used during the training phase.

3.1. Messidor Dataset

The Messidor dataset [26], was collected from three ophthalmologic stations utilizing a digital video recording camera mounted on a Topcon TRC NW6, which is specifically a non-mydratic retinograph with the specification of a 45-degree field of view to collect color pictures of 1200 fundus scans.

3.2. Image Pre-Processing

The adaptive wiener filter [27] uses a filtering method to remove the noise which occurs from the manual function, machine vibration and image reconstruction. It optimizes images and assists to examine contour location in an accurate way. The adaptive wiener filter can effectively preserve image edge and reduce noise through the filter. The regional average and variance is used in the estimation by substituting the gray level. The regional average is formulated by,

$$b = \frac{1}{CD} \sum_{k_1, k_2 \in K} G(k_1, k_2) \quad (1)$$

where, C and D are the length and width of windows, K indicates the value of inputted image selected in window size, k_1, k_2 is coordinates of the original image chosen though the size of the window, and G refers to the input image.

The variance is represented by,

$$\sigma^2 = \frac{1}{CD} \sum_{k_1, k_2 \in K} G^2(k_1, k_2) - b^2 \quad (2)$$

where, b refers to the regional average. The coordinates are expressed by,

$$f(k_1, k_2) = b + \frac{\sigma^2 - q^2}{\sigma^2} (G(k_1, k_2) - b) \quad (3)$$

where, q^2 is noise variance. Hence, the image pre-processed B_g is subjected to the tumor segmentation process.

1) 3.3. Network architecture

In this work, we propose a novel 3D dual-domain attention module (DDA3D) shown in Fig 2 attached in the encoding stages of DynNet backbone to learn global and local information by residual attention learning [14]. The key insight in DDA3D is to build the spatial-domain block S and the decoder-block D as an UNet backbone focusing on local details from voxel-to-voxel. In contrast, the context-domain block C has more profound layers of learning the global information by a large reception field. Dual-domain fusion based on [15] merges two domains with different spatial resolutions and channel dimensions. The result presents that the encoding feature map using 3D-DDA has a larger receptive field on tumor regions than the case without 3D-DDA.

The overall process is shown in Fig.1. The input data is 4 MRI scans $I \in \mathbb{R}^{h \times w \times d \times 4}$ describing four modalities T1-weighted (T1w), post-contrast T1-weighted with Gadolinium (T1Gd), T2-weighted (T2w), and Fluid Attenuated Inversion Recovery (FLAIR). Our goal is to classify every voxel $p = (x, y, z)$ in I whether p is a whole tumor (WT), tumor core (TC), enhancing tumor (ET), or background. The segmentation output is denoted by $F \in \mathbb{R}^{h \times w \times d \times 4}$.

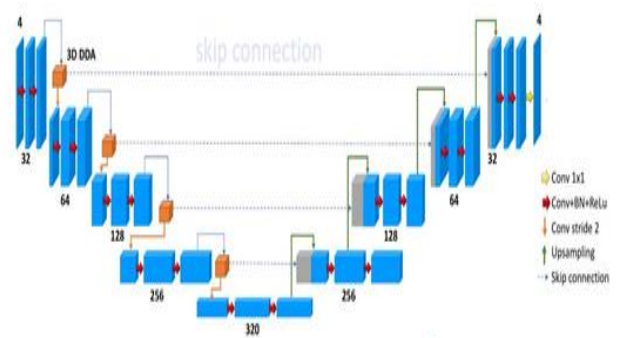


Fig. 1: DynUNet

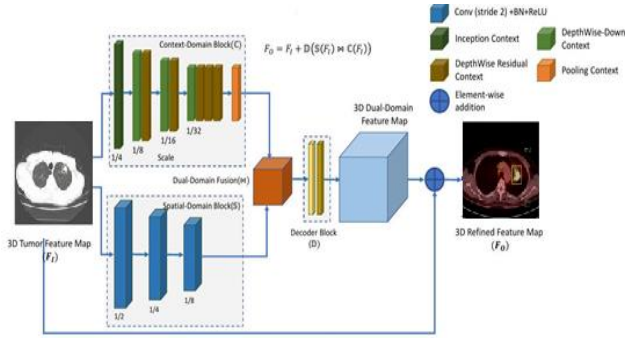


Fig. 2: 3D Dual-Domain Attention

3D-DDA Module. The module is attached at the encoding stage to produce refined feature maps for transferring to the next encoding and corresponding decoding stages. Our proposed module uses residual learning [14] to exploit the local and global domains of the encoding feature map $\mathbf{F}_I \in \mathbb{R}^{w \times h \times d \times c}$ and produce the refined map $\mathbf{F}_O \in \mathbb{R}^{w \times h \times d \times c}$:

$$\mathbf{F}_O = \mathbf{F}_I + \text{DDA3D}(\mathbf{F}_I) \quad (4)$$

where the element-wise multiplication is denoted by \otimes .

$$\text{DDA3D}(\mathbf{F}_I) = \varphi_s(\mathbb{D}(\mathbb{S}(\mathbf{F}_I) \otimes \mathbb{C}(\mathbf{F}_I))) \quad (5)$$

where φ_s is the scale operator by s factor, the dual-domain fusion (\otimes) merges \mathbb{S} and \mathbb{C} to transform to 3D Dual-Domain Feature Map by the decoder block \mathbb{D} . 3D Spatial-Domain block (\mathbb{S}). There are k stacking blocks f in \mathbb{S} , where every block consists of the convolution 3D layer $3 \times 3 \times 3$ Conv3D, the batch normalization layer BN, and ReLU unit σ :

$$\begin{aligned} \mathbb{S}(f_I) &= f_k \circ f_{k-1} \circ \dots \circ f_1(\mathbf{F}_I), \\ f_i &= \sigma(\text{BN}(\text{ConvD}_{s=2}(\mathbf{x}))) \end{aligned} \quad (6)$$

Where k is the number of stacking blocks \mathbb{S} adjusting based on encoding stages, and \circ is the stacking layer operator. The spatial-domain maps are down-sampled by stride 2 in the convolution layer to keep more information details.

3D Context-Domain block (\mathbb{C}). Inspired by semantic blocks in [15] and attention layers [32], we expand these blocks to a 3D version and apply them in 3D Context Domain blocks f_i by stacking sequentially three blocks: the Inception context g_{inc} , Depth wise-

down Context g_{down} , and Depth wise-residual Context g_{res} blocks to learn global information from the encoding intermediate feature map.

$$\begin{aligned} \mathbb{C}(f_I) &= g_{\text{pool}}(f_1 \circ \dots \circ f_{k-1} \circ g_{\text{inc}}(\mathbf{F}_I)), \\ f_i(\mathbf{x}) &= g_{\text{res}_{t-1}} \circ \dots \circ g_{\text{res}_1} \circ g_{\text{down}}(\mathbf{x}) \end{aligned} \quad (7)$$

where g_{pool} is the pooling context block at the last stage to embed global context information with the global average pooling operator, k is the number of context blocks that is larger than the in the spatial domain, and t is the number of residual blocks in the depth wise-down context block. The motivation behind in g_{down} is inspired by the Inception architecture [33], which helps our model to reduce computational costs and produce an effective feature representation. g_{down} and g_{res} employ Conv3D+BN+ReLU layer to transform local feature into higher-dimensional context domain space during down-sampling of the spatial resolution.

Dual-Domain Fusion (\otimes). The block is based on the bilateral block [15] to merge two domains with different resolutions. At every branch, the channel representation is to learn by the depth-wise Conv3D $3 \times 3 \times 3$ followed by Conv3D $1 \times 1 \times 1$, while the spatial representation is to exploit the local details by the Conv3D $3 \times 3 \times 3 + \text{BN}$ followed by the average pooling in the spatial branch and the upsampling layer in the context branch.

3D Decoder block (\mathbb{D}). The block involves three transposed convolution layers with batch normalization and ReLU unit, followed by Conv3D $1 \times 1 \times 1$. The dual-domain feature map is decoded and normalized to transform it to the same size as the input feature map's size.

IV. RESULTS AND DISCUSSION

4.1 Implementation

Experimental results are obtained by implementing a hybrid ResNet50 with melody optimization in Python on an Intel Pentium Core i5 processor with 16GB of RAM and a Windows 7

operating system. The dataset was randomly split into three subsets, with 84, 20, and 30 subjects for training, validation, and testing respectively. The proposed method was trained on an NVIDIA 1080Ti GPU, with 11GB of RAM for 100 epochs.

For quantitative analysis of the experimental results, several performance metrics are considered, including accuracy (AC), sensitivity (SE), specificity (SP), F1-score, Precision and F1-Score. To do this we also use the variables True Positive (TP), True Negative (TN), False Positive (FP), and False Negative (FN). The sensitivity is calculated using Eq. (9) and overall accuracy is calculated using Eq. (11).

$$\text{Precision} = \frac{TP}{TP+FP} \quad (8)$$

$$\text{Sensitivity} = \frac{TP}{TP+FN} \quad (9)$$

$$\text{Specificity} = \frac{TN}{TN+FP} \quad (10)$$

$$\text{Accuracy} = \frac{TP+TN}{TP+TN+FP+FN} \quad (11)$$

$$\text{F1 - Score} = 2 \times \frac{\text{Precision} \times \text{Recall}}{\text{Precision} + \text{Recall}} \quad (12)$$

Where TP, FN, TN, and FP refer to a true positive, false negative, true negative, and false positive respectively.

Fundus images of normal (background retinopathy), mild NPDR, moderate NPDR, severe NPDR, PDR, PDR with new vascularization, and PDR with PLM and with vitreous hemorrhage. Abbreviations: PDR, proliferative diabetic retinopathy; NPDR, nonproliferative diabetic retinopathy; PLM, previous laser marks.

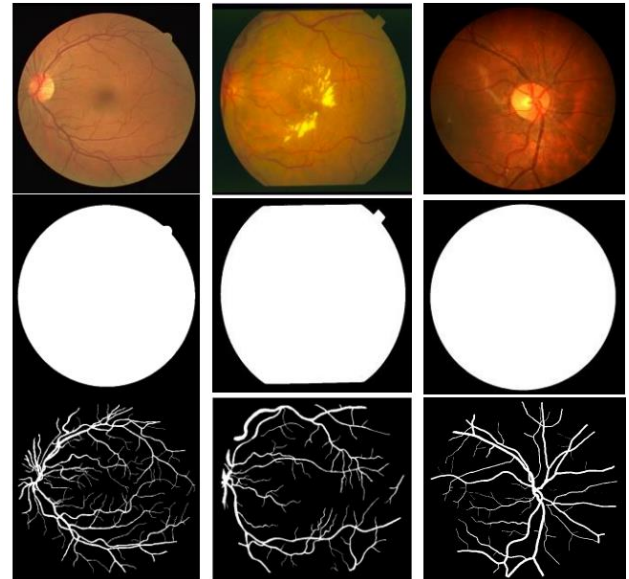


Figure 3 a) Input Image b)Fields of view c) Target Output

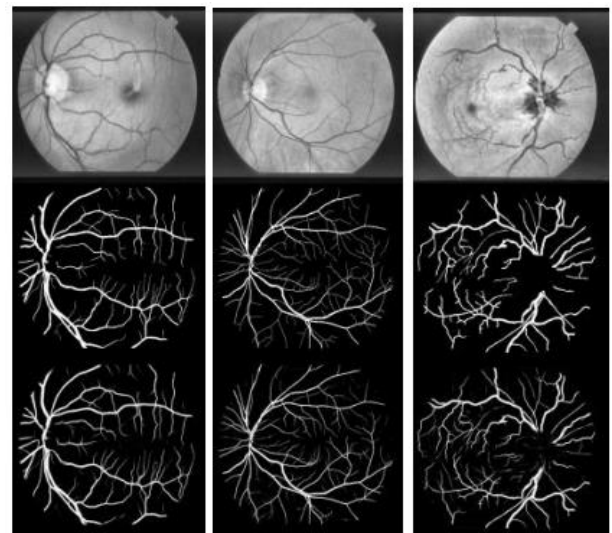


Fig.4. Experimental outputs: a) input image in gray scale, b) ground truth, and c) experimental outputs.

Fig.3 shows the results obtained from Diabetic Retinopathy Detection Using a Deep learning based hybrid Approach. The results obtained depict the fields of view and the targeted output. Fig.4 shows the results obtained from Diabetic Retinopathy. The results obtained depict the input image in gray scale, the ground truth and the output.

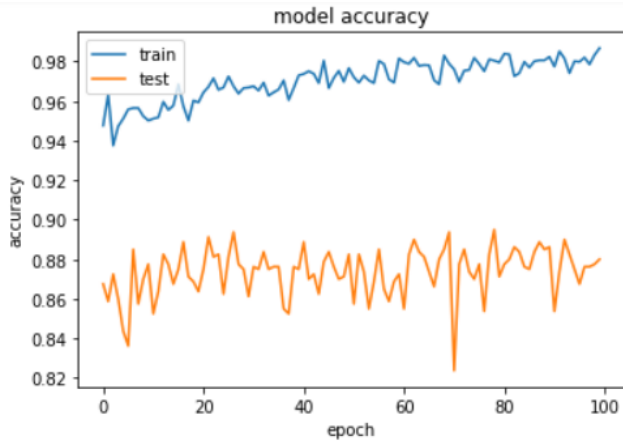


Fig.7 Accuracy Graph

Table 2 Performance of the model.

Architect ure	Accur acy (%)	F1 score	Precisi on	Sensiti vity	Loss
ResNet 50	93.67	0.7068	0.7035	0.7253	0.6034
ResNet 152	94.40	0.7287	0.7141	0.7635	0.5605
Squeezen et 1	91.94	0.6501	0.6347	0.6817	0.8058
Proposed Method	98.65	0.9134	0.9234	0.9454	0.4873

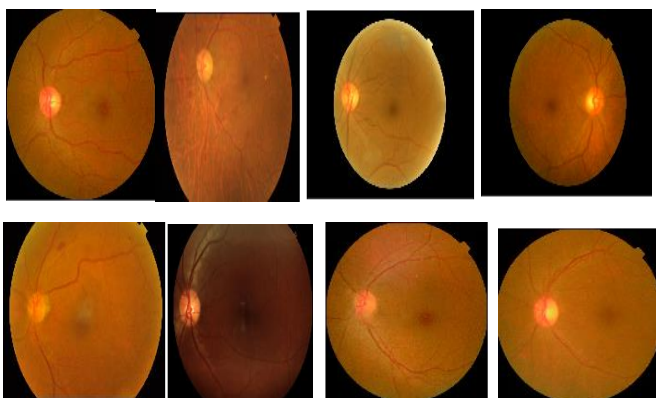
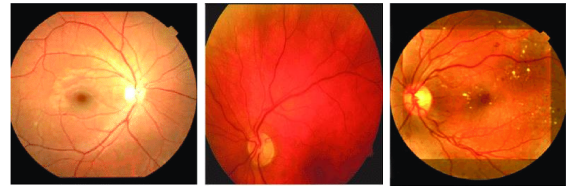


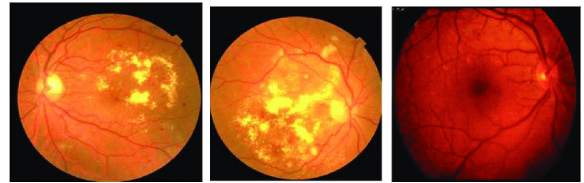
Fig.5. Diabetic Retinopathy identification Using a Deep learning based hybrid Approach

Fig.5 shows the results obtained from Diabetic Retinopathy Detection Using a Deep learning based

hybrid Approach. The results obtained depict the severity of detected retinopathy disease.



a)Without DR b)Early diabetic Retinopathy c)Mild NPDR



d)Moderate NPDR e)Severe NPDR f)PDR and Neovascularization

Fig.6. Diabetic Retinopathy Detection based on categories

Fig.6 shows the Fundus images of normal (background retinopathy), mild NPDR, moderate NPDR, severe NPDR, PDR, PDR with new vascularization, and Abbreviations: PDR, proliferative diabetic retinopathy; NPDR, nonproliferative diabetic retinopathy; PLM, previous laser marks.

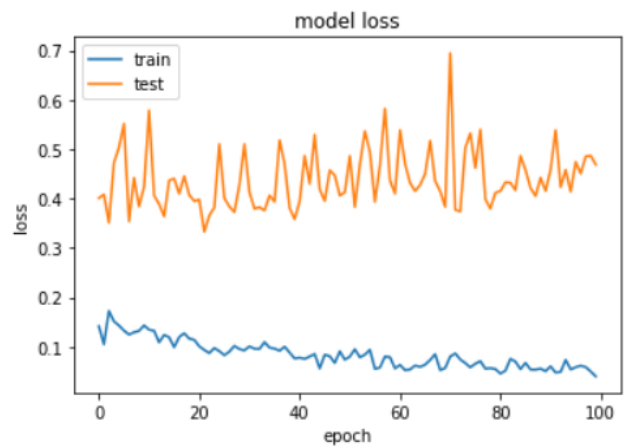


Fig.8 Loss Graph

Fig.7 shows the accuracy graph depicts a steady increase in training accuracy of our approach. Fig.8 shows the loss graph depicts a steady decrease in training loss of our approach.

V. CONCLUSION

DR is one of the common chronic complications of diabetes. Due to the different stage of DR severity, it can be divided into five stages from mild to severe. This paper presented a 3D dual-domain attention module attached at every encoding stage of DynNet for the automatic identification multiple retinal lesions of DR. The model is trained and tested on publicly available Messidor fundus image datasets. The experimental results show that the proposed network can identify the DR stages with high accuracy. The proposed method attains an accuracy of 98.95%, F1-score of 91.34, precision of 94.34, sensitivity of 94.54%, and loss of 0.4873 on the healthy retina, stage 1, stage 2, and stage 3 fundus images. Compared with other models, our proposed network achieves comparable performance. These findings showed the effectiveness and accuracy of our model for CFPs analysis; therefore, it can be implemented in daily clinical practice and to support large-scale robust screening programs for early detection of DR. However, due to the limited number of publicly accessible large training fundus image datasets with multiple identified lesion labels to support multi-label training, future work will be to perform further experiments on larger datasets for more reliable predictions.

VI. REFERENCES

1. Lin X, Yufeng X, Pan X, Jingya X, Ding Y, Sun Xue, Song Xiaoxiao, Ren Yuezhong, Shan Peng-Fei (2020) Global, regional, and national burden and trend of diabetes in 195 countries and territories: an analysis from 1990 to 2025. *Sci Rep* 10(1):1–11
2. Solomon, S.D.; Chew, E.; Duh, E.J.; Sobrin, L.; Sun, J.K.; VanderBeek, B.L.; Wyckoff, C.C.; Gardner, T.W. Diabetic retinopathy: A position statement by the American diabetes association. *Diabetes Care* 2017, 40, 412–418.
3. Bora, A.; Balasubramanian, S.; Babenko, B.; Virmani, S.; Venugopalan, S.; Mitani, A.; Oliveira Marinho, G.D.; Cuadros, J.; Ruamviboonsuk, P.; Corrado, G.S. et al. Predicting the risk of developing diabetic retinopathy using deep learning. *Lancet Digit. Health* 2021, 3, e10–e19.
4. Islam, M.T.; Al-Absi, H.R.; Ruagh, E.A.; Alam, T. DiaNet: A deep learning based architecture to diagnose diabetes using retinal images only. *IEEE Access* 2021, 9, 15686–15695.
5. Arifur, A.M.; Ahmed, J. Automated detection of diabetic retinopathy using deep residual learning. *Int. J. Comput. Appl.* 2020, 177, 25–32.
6. Samanta A, AheliSaha SCS, Steven LF, Yo-Dong Z (2020) Automated detection of diabetic retinopathy using convolutional neural networks on a small dataset. *Pattern Recognit Lett* 2020(04):026.
7. Zeng, X.; Chen, H.; Luo, Y.; Ye, W. Automated diabetic retinopathy detection based on binocular siamese-like convolutional neural network. *IEEE Access* 2019, 7, 30744–30753.
8. Ceylan, M.; Yasar, H. A novel approach for automatic blood vessel extraction in retinal images: Complex ripplelet-I transform and complex valued artificial neural network. *Turk. J. Electr. Eng. Comput. Sci.* 2016, 24, 3212–3227.
9. Chen, X.; Xie, Q.; Zhang, X.; Lv, Q.; Liu, X.; Rao, H. Nomogram Prediction Model for Diabetic Retinopathy Development in Type 2 Diabetes Mellitus Patients: A Retrospective Cohort Study. *J. Diabetes Res.* 2021, 2021, 3825155.
10. Musleh, S.; Alam, T.; Bouzerdoum, A.; Belhaouari, S.B.; Baali, H. Identification of potential risk factors of diabetes for the qatari population. In *Proceedings of the 2020 IEEE International Conference on Informatics, IoT, and Enabling Technologies (ICIOT)*, Doha, Qatar, 2–5 February 2020; pp. 243–246.
11. Mo W, Xiaoshu L, Yexiu Z, Wenjie J (2019)

- Image recognition using convolutional neural network combined with ensemble learning algorithm. *J Phys Conf Ser* 1237(2):022026
12. Samanta A, AheliSaha SCS, Steven LF, Yo-Dong Z (2020) Automated detection of diabetic retinopathy using convolutional neural networks on a small dataset. *Pattern Recognit Lett* 2020(04):026.
 13. Shiva SR, NilambarSethi RR, Gadiraju M (2020) Extensive analysis of machine learning algorithms to early detection of diabetic retinopathy. *Mater Today Proc.* <https://doi.org/10.1016/j.matpr.2020.10.894> (ISSN 2214-7853)
 14. Gaurav S, Dhirendra KV, Amit P, Alpana R, Anil R (2020) Improved and robust deep learning agent for preliminary detection of diabetic retinopathy using public datasets. *Intell Based Med* 3–4:100022. <https://doi.org/10.1016/j.ibmed.2020.100022> (ISSN 2666-5212)
 15. Alyoubi WL, Shalash WM, Abulkhair MF (2020) Diabetic retinopathy detection through deep learning techniques: a review. *Inf Med Unlocked* 20:00377.
 16. Mohsin Butt M, Ghazanfar L, Awang Iskandar DNF, Jaafar A, Adil HK (2019) Multi-channel convolutions neural network based diabetic retinopathy detection from fundus images. *Procedia Comput Sci* 163:283–291.
 17. Islam MM, Yang H-C, Poly TN, Jian W-S, Li Y-C (2020) Deep learning algorithms for detection of diabetic retinopathy in retinal fundus photographs: a systematic review and meta-analysis. *Comput Methods Prog Biomed* 191:105320.
 18. Shanthi, T.; Sabeenian, R.S. Modified alexnet architecture for classification of diabetic retinopathy images. *Comput. Electr. Eng.* **2019**, *76*, 56–64.
 19. Shailesh K, Abhinav A, Basant K, Amit KS (2020) An automated early diabetic retinopathy detection through improved blood vessel and optic disc segmentation. *Opt Laser Technol* 121:66–70
 20. Jaafar HF, Nandi AK, Al-Nuaimy W (2011) Automated detection and grading of hard exudates from retinal fundus images. In: *Proceedings of 19th European signal processing conference*
 21. Casanova R, Saldana S, Chew EY, Danis RP, Greven CM, Ambrosius WT (2014) Application of random forests methods to diabetic retinopathy classification analyses. *PLoS One* 9(6):178–193
 22. Quellec G, Charrière K, Boudi Y, Cochener B, Lamard M (2017) Deep image mining for diabetic retinopathy screening. *Med Image Anal* 39:178–193
 23. Kaggle (2015) Diabetic retinopathy detection. <https://www.kaggle.com/c/diabeticretinopathy-detection/>. Accessed 7 May 2018
 24. Gulshan V et al (2016) Development and validation of a deep learning algorithm for detection of diabetic retinopathy in retinal fundus photographs. *JAMA* 316(22):2402–2410
 25. Gargeya R, Leng T (2017) Automated identification of diabetic retinopathy using deep learning. *Ophthalmology* 124(7):962–969
 26. Messidor-ADCIS. Available online: <http://www.adcis.net/en/thirdparty/messidor/> (accessed on 22 November 2021).
 27. Hardie, Russell. "A fast image super-resolution algorithm using an adaptive Wiener filter." *IEEE Transactions on Image Processing* 16.12 (2007): 2953-2964.
 28. Ronneberger, Olaf, Philipp Fischer, and Thomas Brox. "U-net: Convolutional networks for biomedical image segmentation." *Medical Image Computing and Computer-Assisted Intervention–MICCAI 2015: 18th International Conference, Munich, Germany, October 5-9, 2015, Proceedings, Part III* 18. Springer International Publishing, 2015.

29. He, K., Zhang, X., Ren, S., and Sun, J. (2016). "Deep residual learning for image recognition," in IEEE Conference on Computer Vision and Pattern Recognition (Las Vegas, NV), 770–778. doi: 10.1109/CVPR.2016.90
30. Wang, Jun, et al. "Prior-attention residual learning for more discriminative COVID-19 screening in CT images." IEEE transactions on medical imaging 39.8 (2020): 2572-2583.
31. Duan, Shuchao, et al. "Multi-scale gradients self-attention residual learning for face photo-sketch transformation." IEEE Transactions on Information Forensics and Security 16 (2020): 1218-1230.
32. Lou, Ange, Shuyue Guan, and Murray Loew. "Cfpnet-m: A light-weight encoder-decoder based network for multimodal biomedical image real-time segmentation." Computers in Biology and Medicine 154 (2023): 106579.
33. Shankar, K.; Perumal, E.; Vidhyavathi, R.M. Deep neural network with moth search optimization algorithm based detection and classification of diabetic retinopathy images. Social Netw. Appl. Sci. 2020, 2, 748.
34. Shanthi, T.; Sabeenian, R.S. Modified alexnet architecture for classification of diabetic retinopathy images. Comput. Electr. Eng. 2019, 76, 56–64.

Cite this article as :

Benix Pearlin Moses M, R. Maria Sheeba, "Diabetic Retinopathy Severity Identification Using 3D Dual-Domain Attention Approach", International Journal of Scientific Research in Science and Technology (IJSRST), Online ISSN : 2395-602X, Print ISSN : 2395-6011, Volume 10 Issue 5, pp. 302-311, September-October 2023. Available at doi : <https://doi.org/10.32628/IJSRST52310538>
Journal URL : <https://ijsrst.com/IJSRST52310538>